Tetramerized Structure of $(DMET)_2ReO_4$ and Its Apparent Metallic Behavior in Resistivity

Kazuya SAITO, Yoshimitsu ISHIKAWA, Masayoshi ISHIBASHI, Koichi KIKUCHI, Keiji KOBAYASHI,† and Isao IKEMOTO*

Department of Chemistry, Faculty of Science, Tokyo Metropolitan Unversity, Fukazawa, Setagaya-ku, Tokyo 158

†Department of Chemistry, College of Arts and Sciences, The University of Tokyo, Komaba, Meguro-ku, Tokyo 153

(Received December 26, 1989)

The crystal structure of $(DMET)_2ReO_4$ (DMET: 5,6-dihydro-2-(4,5-dimethyl-1,3-diselenol-2-ylidene)dithiolo[4,5-*b*][1,4]dithiin) was determined, and its resisitivity and thermoelectric power were measured. Crystal data; $(C_{10}H_{10}S_4Se_2)_2 \cdot ReO_4$, M_r=1082.88, triclinic, $P\bar{1}$, a=6.715(1) Å, b=14.486(2) Å, c=15.867(2) Å, α=101.95(4)°, β=90.05(1)°, γ=78.43(1)°, V=1478.2(3) Å^3, Z=2, D_x=2.43 Mg m^{-3}, μ(Mo $K\alpha$)=9.62 mm^{-1}, $F(000)$=1022, T=297 K, R=0.074 for 4391 reflections. The crystal has columnar structure. In the column, a large degree of tetramerization is observed. The resistivity under the normal pressure has metallic temperature dependence above ca. 295 K. The thermoelectric power is essentially constant above 200 K and no anomaly was detected around 295 K. The apparent metallic behavior was attributed to the small activation energy (band-gap) and the temperature dependence of the carrier mobility.

DMET is the first of the unsymmetrical donors the radical salt(s) of which show the superconductivity.[1-6] The molecule consists of halves of TMTSF and BEDT-TTF molecules (Fig. 1). A wide variety in crystal structure[5,7-13] and physical properties,[14-22] including the superconductivity,[1-5] has been demonstrated in the DMET family. The family has been classified into five groups on the basis of the shape of anions and electrical properties.[15,17] Each group has the characteristic crystal structure.[11] According to the classification scheme, the title compound, $(DMET)_2ReO_4$, seems to belong to group 2, which includes BF_4 and ClO_4 salts, because the shape of the anion has the tetrahedral symmetry. No direct confirmation of the prospect, however, has been made so far. The situation prompted us to start the study on the crystal structure and electrical properties of $(DMET)_2ReO_4$. The apparent inconsistency between the structure and the electrical properties are discussed.

Experimental

Sample. DMET was synthesized according to the method described previously.[23,24] Crystals of $(DMET)_2ReO_4$ were prepared by electrochemical oxidation of DMET in chlorobenzene solution in the presence of $(n\text{-}Bu_4N)ReO_4$ at a constant current (1 μA).

Crystal Structure Analysis. A black plate-like crystal 0.21×0.13×0.03 mm^3. D_m not determined. Rigaku AFC-M automated four-circle diffractometer. Unit-cell dimensions determined from 20 selected reflections ($27° < 2\theta < 31°$). Intensity data collected using the ω-2θ scan technique ($\Delta\omega = 1.30° + 0.14° \cdot \tan\theta$) with a scan rate 4° min^{-1} in ω to $(\sin\theta)/\lambda$=0.65 Å^{-1} ($-8 \leqslant h \leqslant 8$, $-18 \leqslant k \leqslant 18$, $0 \leqslant l \leqslant 20$). Three standard reflections measured at an interval of 100 reflections, small (<1.7%) random variations. Data corrected for absorption effects using a Gaussian integration procedure; T_{min}=0.20, T_{max}=0.77. 7026 indepencdent reflections collected; 4391 reflections ($|F_o| > 3\sigma(F_o)$) used in the structure refinement. Intensity statistics indicated space group $P\bar{1}$ rather than P1 and this choice was later confirmed by the successful structure solution and least-squares refinement. Structure solved by the Patterson and the heavy atom methods and refined by the block-diagonal least-squares method. Atomic and anomalous scattering factors from International Tables for X-ray Crystallography.[25] All computations carried out using UNICS III program.[26] H atoms not located. $\Sigma w \cdot (|F_o| - |F_c|)^2$ minimized, where $w = \{\sigma^2(|F_o|) + 0.0088 \cdot |F_o|^2\}^{-1}$, with $\sigma(|F_o|)$ based on counting statistics. $(\Delta/\sigma)_{max}$=0.02 for B_{33} of Re(1) in final least-squares cycle which resulted in the agreement factors R=0.074, wR=0.103 and S=0.82. No correction for secondary extinction. A difference synthesis based on the structure factors derived from the final parameter values showed some peaks of density (−3.3—3.2 $e \cdot$Å^{-3}). ORTEP II[27] was used to produce crystal structure illustrations.

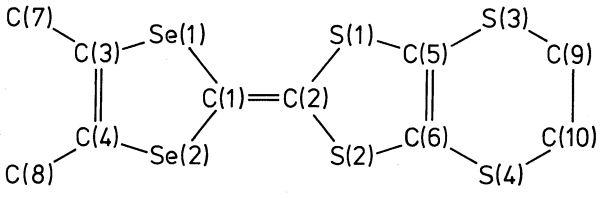

Fig. 1. Numbering scheme for DMET molecule.

Resistance and Thermoelectric Power Measurements. The resistance was measured of some samples using the AC (20 Hz) four-probe method at constant current of 10 μA between 80 and 325 K. Pressure was generated using a pressure-cell of clamp type, in which oil (Daphne #7373, Idemitsu Oil Co., Ltd.) was used as pressure medium. The actual pressure in the cell was monitored by measuring the resistance of a manganin wire as a pressure sensor. The pressure in the cell varies on cooling (heating) due to the difference in the thermal contraction (expansion) between the cell and pressure medium. The measurements were made under every ca. 0.1 kbar (1 bar=10^5 Pa) from the normal pressure to 0.8 kbar. The results were interpolated and the values at rounded temperatures and pressures were

estimated.

The thermoelectric power under the normal pressured was measured of some samples between liquid nitrogen and room temperatures by the method decribed elsewhere.[22] The measurements under pressures were performed between 270 and 320 K from the normal pressure to 0.6 kbar using a newly constructed sample holder in the same pressure-cell as in the resistance measurements. The principle and the operation of the new apparatus is essentially the same as in the case of the normal pressure.[22] The details of the sample holder will be published shortly.[28] The pressure correction was not applied for the results of the thermoelectric power measurements because of rather narrow temperature range of the measurements. Since the calibration of the apparatus has not been completed, the values of the data points under pressures are not absolute thermolectric power though they may be not far from the true value.

Results

Crystal Structure. The crystal structure at 297 K viewed along the *a* axis is shown in Fig. 2. There are two independent DMET molecules (A and B). The numbering scheme is given in Figs. 1 and 2. The final positional and thermal parameters are tabulated in Table 1 and the bond lengths and angles in Tables 2 and 3.[29] The geometry of the DMET molecules is in reasonable agreement with those observed in other DMET salts.[7,10,12,13] Both of molecules A and B are almost planar except for the ethylenedithio group in contrast to neutral DMET molecule.[30] The C(10A) and C(10B) atoms are away by 0.7 and 0.8 Å, respectively, from the molecular plane determined with two selenium, two inner sulfur, and central carbon atoms. The other atoms are within about 0.1 Å from the

Table 1. Fractional Atomic Coordinates and Equivalent Isotropic Thermal Factors of $(DMET)_2ReO_4$

Atom	$10^3 \cdot x$	$10^4 \cdot y$	$10^4 \cdot z$	B_{eq}[a]/Å^2
Molecule A				
Se(1)	274.6(2)	1690(1)	5585(1)	2.28(3)
Se(2)	747.8(2)	1141(1)	5140(1)	2.22(3)
S(1)	203.5(5)	839(3)	3524(2)	2.4(1)
S(2)	642.8(5)	351(3)	3111(2)	2.3(1)
S(3)	80.5(6)	143(3)	1777(3)	3.3(1)
S(4)	607.7(6)	−446(3)	1260(2)	3.3(1)
C(1)	485(2)	1179(10)	4744(8)	2.2(3)
C(2)	446(2)	849(10)	3906(8)	2.1(3)
C(3)	454(2)	1911(9)	6504(8)	2.2(3)
C(4)	656(2)	1675(9)	6305(9)	2.1(3)
C(5)	284(2)	320(9)	2450(8)	2.3(3)
C(6)	485(2)	94(9)	2251(8)	1.8(3)
C(7)	352(3)	2348(10)	7370(8)	3.1(4)
C(8)	825(2)	1821(11)	6911(10)	3.0(4)
C(9)	210(3)	−278(13)	724(10)	3.7(5)
C(10)	408(3)	−1018(13)	709(11)	4.2(5)
Molecule B				
Se(1)	680.8(2)	3004(1)	3585(1)	2.32(3)
Se(2)	208.0(2)	3548(1)	4022(1)	2.29(3)
S(1)	749.3(5)	3859(3)	5654(2)	2.5(1)
S(2)	309.7(5)	4353(2)	6047(2)	2.3(1)
S(3)	868.6(6)	4461(3)	7420(2)	3.0(1)
S(4)	340.3(5)	5050(3)	7918(2)	2.8(1)
C(1)	470(2)	3547(9)	4428(9)	2.3(3)
C(2)	505(2)	3869(9)	5252(9)	2.2(3)
C(3)	502(2)	2781(10)	2672(9)	2.5(4)
C(4)	302(2)	2990(9)	2866(8)	2.1(3)
C(5)	673(2)	4320(9)	6733(8)	1.9(3)
C(6)	468(2)	4553(10)	6911(9)	2.6(4)
C(7)	604(3)	2324(13)	1796(10)	3.6(5)
C(8)	135(2)	2820(11)	2234(9)	2.8(4)
C(9)	734(3)	5022(15)	8442(11)	4.8(6)
C(10)	544(3)	4762(19)	8657(13)	5.7(7)
ReO_4				
Re(1)	34.5(1)	2922(1)	−222.5(4)	3.82(2)
O(1)	−114(2)	3877(11)	461(11)	7.0(5)
O(2)	−80(4)	2690(13)	−1148(12)	9.4(7)
O(3)	79(4)	1945(13)	205(10)	10.1(8)
O(4)	260(4)	3207(21)	−401(22)	14.0(13)

a) $B_{eq}=(4/3)\cdot(B_{11}\boldsymbol{a}\cdot\boldsymbol{a}+B_{12}\boldsymbol{a}\cdot\boldsymbol{b}+B_{13}\boldsymbol{a}\cdot\boldsymbol{c}+\cdots)$.

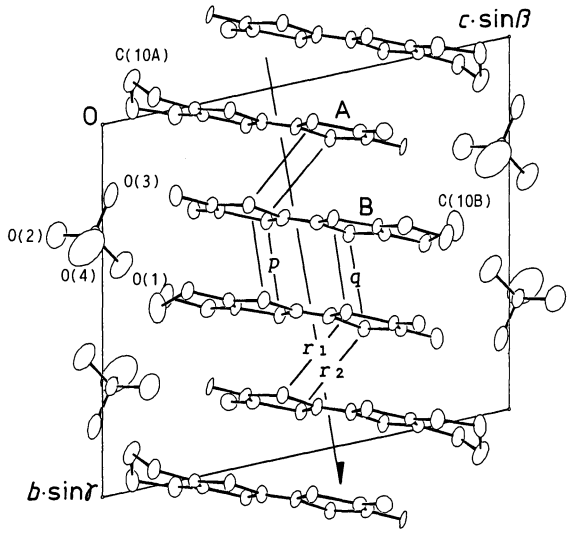

Fig. 2. Crystal structure of $(DMET)_2ReO_4$ viewed along the *a* axis. Thermal ellipsoids indicate the region of 50% probability. Thin solid lines show the shorter intermolecular contacts than the sum of van der Waals radii. Their distances; p=3.754(4) Å, q=3.766(4) Å, r_1=3.984(2) Å, and r_2=3.979(2) Å. The arrow indicates the "stacking axis" of a tetramer.

corresponding plane. The anion ReO_4 is ordered and located at a general point.

As seen in Fig. 2, the DMET molecules are arranged in an ordered stack along the *b* axis and the basic period of the crystal lattice contains four molecules. The structure is different from those of $(DMET)_2BF_4$ and $(DMET)_2ClO_4$ in spite of the same shape of the anions.[11] Although molecules A and B are independent from each other, they are almost parallel within 0.1°. The normals of the molecular planes, determined with six central atoms, are tilted by ca. 11° from the *b* axis. The interplanar distances are 3.60(1), 3.53(1) and 3.54(1) Å for pairs of molecules A–A, B–B, and A–B, respectively. The rather large distance for the A–A pair suggests the tetramerized structure. The solid lines in Fig. 2 indicate the shorter interatomic contacts than the sum of van der Waals radii. The short contacts in the direction of the *b* axis are confined within a "tetramer". The stacking mode is quite normal within a tetramer. The situation is clearly seen in Fig. 3. While the projection of a DMET column along the crystallographic axis (*b* axis) is

Table 2. Bond Lengths (l)

Bond	l/Å	l/Å	Bond	l/Å	l/Å
DMET	Molecule A	Molecule B		Molecule A	Molecule B
Se(1)-C(1)	1.87(1)	1.88(1)	S(3) -C(9)	1.81(2)	1.81(2)
Se(1)-C(3)	1.91(1)	1.90(1)	S(4) -C(6)	1.73(1)	1.76(1)
Se(2)-C(1)	1.87(1)	1.87(1)	S(4) -C(10)	1.84(2)	1.84(2)
Se(2)-C(4)	1.90(1)	1.90(1)	C(1) -C(2)	1.36(2)	1.33(2)
S(1) -C(2)	1.74(1)	1.76(1)	C(3) -C(4)	1.35(2)	1.33(2)
S(1) -C(5)	1.75(1)	1.74(1)	C(3) -C(7)	1.49(2)	1.51(2)
S(2) -C(2)	1.76(1)	1.75(1)	C(4) -C(8)	1.51(2)	1.53(2)
S(2) -C(6)	1.75(1)	1.75(2)	C(5) -C(6)	1.35(2)	1.37(2)
S(3) -C(5)	1.76(2)	1.72(1)	C(9) -C(10)	1.53(2)	1.46(3)
ReO_4					
Re(1)-O(1)	1.71(1)		Re(1)-O(3)	1.67(2)	
Re(1)-O(2)	1.66(2)		Re(1)-O(4)	1.68(3)	

Table 3. Bond Angles (θ)

Angle	θ/°	θ/°	Angle	θ/°	θ/°
DMET	Molecule A	Molecule B		Molecule A	Molecule B
C(1) -Se(1) -C(3)	94.2(5)	94.2(6)	Se(1)-C(3) -C(7)	115.3(10)	115.2(10)
C(1) -Se(2) -C(4)	93.6(5)	93.9(6)	C(4) -C(3) -C(7)	127.2(13)	126.7(13)
C(2) -S(1) -C(5)	95.9(6)	97.1(6)	Se(2)-C(4) -C(3)	119.2(10)	119.3(10)
C(2) -S(2) -C(6)	96.4(6)	96.3(6)	Se(2)-C(4) -C(8)	113.6(9)	114.7(9)
C(5) -S(3) -C(9)	101.8(7)	102.5(8)	C(3) -C(4) -C(8)	127.1(12)	126.0(11)
C(6) -S(4) -C(10)	100.5(7)	101.2(8)	S(1) -C(5) -S(3)	112.9(8)	115.0(7)
Se(1)-C(1) -Se(2)	115.4(6)	114.4(7)	S(1) -C(5) -C(6)	118.1(10)	115.9(10)
Se(1)-C(1) -C(2)	121.3(9)	122.6(10)	S(3) -C(5) -C(6)	129.0(10)	129.1(10)
Se(2)-C(1) -C(2)	123.3(9)	122.9(10)	S(2) -C(6) -S(4)	116.1(7)	114.8(8)
S(1) -C(2) -S(2)	113.9(7)	113.2(7)	S(2) -C(6) -C(5)	115.7(9)	117.4(10)
S(1) -C(2) -C(1)	124.4(9)	123.9(10)	S(4) -C(6) -C(5)	128.2(10)	127.8(11)
S(2) -C(2) -C(1)	121.7(9)	122.9(10)	S(3) -C(9) -C(10)	114.1(12)	120.2(14)
Se(1)-C(3) -C(4)	117.5(10)	118.0(10)	S(4) -C(10)-C(9)	110.9(12)	113.3(17)
ReO_4					
O(1)-Re(1)-O(2)	109.3(9)		O(2)-Re(1)-O(3)	109.7(10)	
O(1)-Re(1)-O(3)	111.3(9)		O(2)-Re(1)-O(4)	109.8(14)	
O(1)-Re(1)-O(4)	108.7(11)		O(3)-Re(1)-O(4)	108.0(15)	

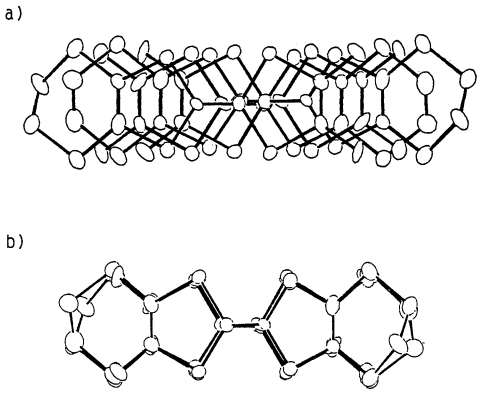

Fig. 3. Overlap mode. a; tetramer in $(DMET)_2ReO_4$ viewed along the *b* axis, b; tetramer in $(DMET)_2ReO_4$ viewed along the "stacking axis" of the tetramer (indicated with an arrow in Fig. 2).

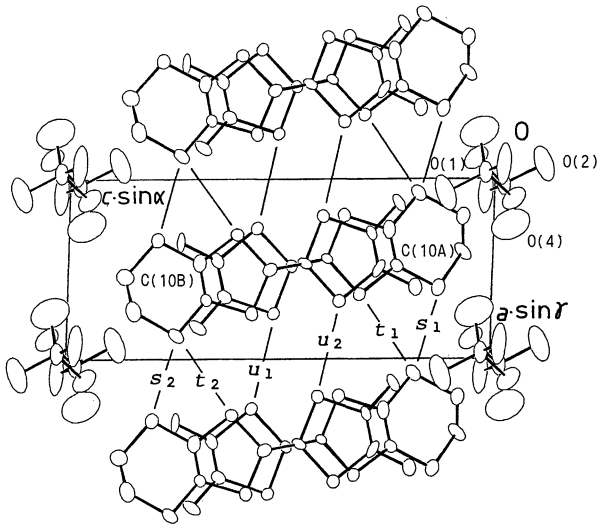

Fig. 4. Crystal structure of $(DMET)_2ReO_4$ viewed along the *b* axis. Two independent DMET molecules, which lie within ca. 0.0—0.5 in *y*, are shown in each column for clarity. Thermal ellipsoids indicate the region of 50% probability. Thin solid lines show the shorter intermolecular contacts than the sum of van der Waals radii. All of the short contacts exist between the molecules related by the translation *a* along the *a* axis. Their distances; s_1= 3.503(6) Å, s_2=3.491(6) Å, t_1=3.551(5) Å, t_2= 3.638(5) Å, u_1=3.813(2) Å, and u_2=3.754(4) Å.

complicated, four molecules overlap in the similar way to those in other DMET salts if we see along the direction drawn in Fig. 2 with an arrow, the "stacking axis" of the tetramer. The normals of the molecular planes are tilted by about 20° from the stacking axis as in the cases of other DMET salts.[10,12,13]

Figure 4 shows the crystal structure of $(DMET)_2ReO_4$ viewed along the *a* axis. There exist three short intercolumnar contacts for molecules A and B, separately. The pattern of the intercolumnar contacts is the same as those observed in other DMET salts.[7,8,10–13]

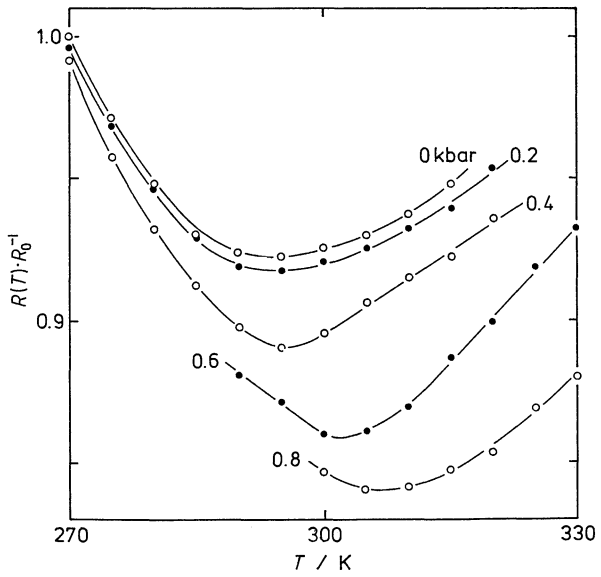

Fig. 5. Resistivity of $(DMET)_2ReO_4$ under pressures. R_0 denotes the resistance at 270 K under the normal pressure, i.e. $R_0=R(T=270\text{ K}, p=1\text{ bar})$.

Electrical Resistance. The resistivity of $(DMET)_2ReO_4$ at room temperature is 40 S cm^{-1} under the normal pressure and gradually increases with increasing pressure as seen in Fig. 5. Although the minimum is very broad, the dependence is seemingly metallic above about 295 K under the normal pressure. The activation energy in the semiconducting region was deduced as 3.9 kJ mol^{-1} from an Arrhenius plot. On applying low pressure, the location of the minimum slightly shifts toward the high temperature side. There exists, however, the metallic region. Although the metal-insulator "transition temperature" is much higher than those in BF_4 and ClO_4 salts, the behavior of ReO_4 salts is consistent with the classification (group 2).[15,17]

Thermoelectric Power. The results of the thermoelectric power measurements under ca. 0.2 kbar are polotted in the region of the metal-insulator "transition" in Fig. 6. The "transition" temperature is about 295 K from Fig. 5. The thermoelectric power is almost independent of temperature and there is nothing anomalous around 295 K. The results under other pressures were essentially the same. It is well-known that thermoelectric power of metal is proportional to temperature. Hence, the results show that $(DMET)_2ReO_4$ is not metallic at the microscopic level and that the "transition" is not a phase transition in thermodynamic sense. The positive value implies that the carrier is hole.

The absolute thermoelectric power under the normal pressure is plotted in Fig. 7 in the wider temperature region. The thermoelctric power is almost independent of temperature with the positive

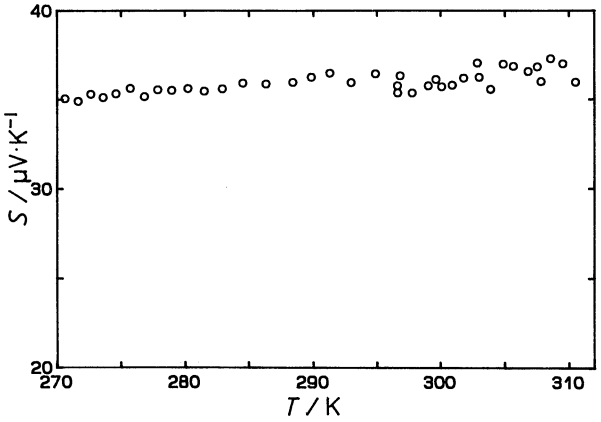

Fig. 6. Thermoelectric power of $(DMET)_2ReO_4$ under about 0.2 kbar.

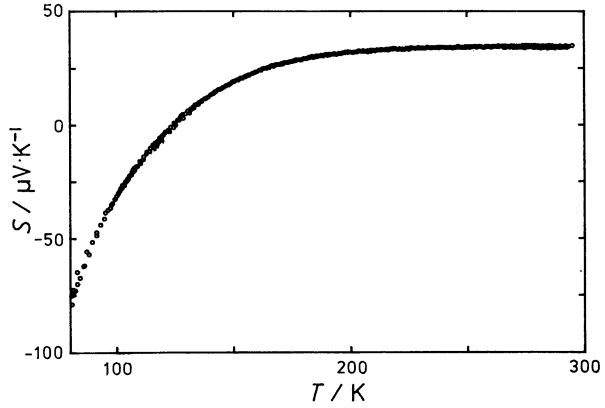

Fig. 7. Absolute thermoelectric power of $(DMET)_2ReO_4$ under the normal pressure.

value of 33 $\mu V\ K^{-1}$ above 200 K, slowly decreases with decreasing temperature, passes zero at about 140 K, and then decreases rapidly with an incresing slope. There is no region where the thermoelectric power is proportional to temperature.

Discussion

The experimental results are summarized as follows: The crystal structure is described as columns of tetramers. The broad minimum appears in the resistivity. No anomaly is detected in thermoelectric power around the temperature of the resistance minimum. The temperature-independent thermoelectric power is observed. Since the period of four DMET molecules corresponds to $2k_F$ distortion from the stoichiometry of the system, the crystal should be insulating, irrespective of the degree of electron correlation. The seemingly metallic behavior observed in the resistivity is in contradiction with the structure.

These results of the resistivity and the thermoelectric power are quite similar to those reported for $(TMTTF)_2ClO_4$,[31] where the apparent "metallic" behavior was attributed to the rather strong temperature dependence in the mobility of charge carriers. We tried the same analysis as $(TMTTF)_2ClO_4$. Temperature dependence of resistivity of semiconductor is generally expressed as,

$$\rho \propto T^{\alpha-0.5}\cdot\exp(-E_a/RT),$$

where E_a is the activation energy, the half of the band-gap in intrinsic semiconductors. α is the exponent characterizing the temperature dependence of the carrier mobility and it depends on the mechanism of the electron scattering. It is observed that, if E_a is small, the resistivity increases with increasing temperature due to the temperature dependence of the mobility. The location of the resistivity minimum is calculated as,

$$T(\rho_{min}) = (E_a/R)\cdot(\alpha - 0.5)^{-1}.$$

Using the value of the activation energy (3.9 kJ mol^{-1}) and the temperature of the resistivity minimum (295 K), the magnitude of α is calculated as 2.0. It is well-known that the simple electron scattering by phonon gives the value 2. The present value of α is, therefore, in a reasonable range. Namely, $(DMET)_2ReO_4$ is intrinsically semiconducting and the apparent metallic behavior is due to the temperature dependence in the mobility of the carriers.

Concerning the temperature-independent thermoelectric power, it is likely that the effect of electron correlation plays an important role. It is well-known that the thermoelectric power is independent of temperature when the ratio betwee the on-site Coulomb repulsion and the transfer integral is sufficiently large, i.e. $U/4t \gg 1$. The expected value is 60 $\mu V\ K^{-1}$ for the quarter-filled hole hand. The observed value (33 $\mu V\ K^{-1}$) is smaller than the expected, but not too small. Thus, it is regarded as an indication of the strong electron correlation. The fact that there is no shorter contact between tetramers along the stacking axis seems to support this conclusion. The smaller value than 60 $\mu V\ K^{-1}$ implies $U/4t$ has a rather large but finite value.[31] Optical measurements will provide a direct evidence for the conclusion, and are in progress.[32]

There remains a problem, that is why the thermoelectric power changes the sign betow 140 K. Similar behavior was also reported for $(TMTTF)_2ClO_4$,[31] where the negative thermoelectric power was attributed to some defects. Although the same explanation may be possible for the present case, this point is open at present.

Since the metal-insulator "transition" in $(DMET)_2ReO_4$ is not a thermodynamic phase transition as demonstrated in the thermoelectric power measure-

ments, the crystal structure at low temperatures must be essentially the same as that determined in this work. On lowering temperature, however, the degree of the tetramerization becomes stronger and stronger, accrding to the enhancement of the electron localization. Since neutral[30] and partially-oxidized[5,7,20-13] DMET molecules have the different geometry, low-temperature X-ray studies may reveal the location of electrons after the electron localization occurs.

In conclusion, $(DMET)_2ReO_4$ has tetramerized structure distinct from any other radical salts of DMET, and is characterized by a rather strong electron correlation. The seemingly metallic behavior in the resistivity is attributed to the small band-gap and the temperature dependence of the carrier mobility.

The authors express their thanks to Professor V. M. Yartsev of Chelyobinsk State University for valuable discussion, to Mr. Hideki Saitoh for his help in preparing manuscripts and to Mr. Harukazu Yoshino for his technical assistance in experiments. This work was supported in part by Grant-in-Aid for Specially Promoted Research (No. 63060004) from the Ministry of Education, Science and Culture.

References

1) K. Kikuchi, M. Kikuchi, T. Namiki, K. Saito, I. Ikemoto, K. Murata, T. Ishiguro, and K. Kobayashi, *Chem. Lett.*, **1987**, 931.

2) K. Kikuchi, K. Murata, Y. Honda, T. Namiki, K. Saito, K. Kobayashi, T. Ishiguro, and I. Ikemoto, *J. Phys. Soc. Jpn.*, **56**, 2627 (1987).

3) K. Kikuchi, K. Murata, Y. Honda, T. Namiki, K. Saito, T. Ishiguro, K. Kobayashi, and I. Ikemoto, *J. Phys. Soc. Jpn.*, **56**, 3436 (1987).

4) K. Kikuchi, K. Murata, Y. Honda, T. Namiki, K. Saito, H. Anzai, K. Kobayashi, and I. Ikemoto, *J. Phys. Soc. Jpn.*, **56**, 4241 (1987).

5) K. Kikuchi, Y. Honda, Y. Ishikawa, K. Saito, I. Ikemoto, K. Murata, H. Anzai, T. Ishiguro, and K. Kobayashi, *Solid State Commun.*, **66**, 405 (1988).

6) G. C. Papavassiliou, G. A. Mousdis, J. S. Zambounis, A. Terzis, A. Hountas, B. Hilti, C. W. Mayer, and J. Pfeiffer, *Synth. Metals*, **27**, B379 (1988).

7) M. Z. Aldoshina, L. O. Atovmyan, L. M. Gol'denberg, O. N. Krasochka, R. N. Lyubovskaya, R. B. Lyubovskii, and M. L. Khidekel', *Dokl. Acad. Nauk S. S. S. R.*, **289**, 1140 (1986).

8) K. Kikuchi, I. Ikemoto, and K. Kobayashi, *Synth. Metals*, **19**, 551 (1987).

9) Y. Nogami, M. Tanaka, S. Kagoshima, K. Kikuchi, K. Saito, I. Ikemoto, and K. Kobayashi, *J. Phys. Soc. Jpn.*, **56**, 3783 (1987).

10) K. Kikuchi, Y. Ishikawa, K. Saito, I. Ikemoto, and K. Kobayashi, *Acta Crystallogr., Sect. C*, **44**, 466 (1988).

11) K. Kikuchi, Y. Ishikawa, K. Saito, I. Ikemoto, and K. Kobayashi, *Synth. Metals*, **27**, B 391 (1988).

12) Y. Ishikawa, K. Kikuchi, K. Saito, I. Ikemoto, and K. Kobayashi, *Acta Crystallogr., Sect. C*, **45**, 572 (1989).

13) Y. Ishikawa, K. Saito, K. Kikuchi, I. Ikemoto, K. Kobayashi, and H. Anzai, *Acta Crystallogr., Sect. C*, in press.

14) K. Kanoda, T. Takahashi, T. Tokiwa, K. Kikuchi, K. Saito, I. Ikemoto, and K. Kobayashi, *Phys. Rev. B*, **38**, 39 (1988).

15) K. Murata, K. Kikuchi, T. Takahashi, K. Kobayashi, Y. Honda, K. Saito, K. Kanoda, T. Tokiwa, H. Anzai, T. Ishiguro, and I. Ikemoto, *J. Mol. Electron.*, **4**, 173 (1988).

16) K. Kanoda, T. Takahashi, K. Kikuchi, K. Saito, I. Ikemoto, and K. Kobayashi, *Synth. Metals*, **27**, B385 (1988).

17) K. Kikuchi, K. Saito, I. Ikemoto, K. Murata, T. Ishiguro, and K. Kobayashi, *Synth. Metals*, **27**, B269 (1988).

18) K. Kanoda, T. Takahashi, K. Kikuchi, K. Saito, Y. Honda, I. Ikemoto, K. Kobayashi, K. Murata, and H. Anzai, *Solid State Commun.*, **69**, 415 (1989).

19) K. Kanoda, T. Takahashi, K. Kikuchi, K. Saito, Y. Honda, I. Ikemoto, and K. Kobayashi, *Phys. Rev. B*, **39**, 3996 (1989).

20) K. Saito, H. Kamio, K. Kikuchi, K. Kobayashi, and I. Ikemoto, *J. Phys.: Condensed Matt.*, **1**, 8823 (1989).

21) Y. Honda, K. Murata, K. Kikuchi, K. Saito, I. Ikemoto, and K. Kobayashi, *Solid State Commun.*, **71**, 1087 (1989).

22) K. Saito, H. Kamio, Y. Honda, K. Kikuchi, K. Kobayashi, and I. Ikemoto, *J. Phys. Soc. Jpn.*, **58**, 4093 (1989).

23) K. Kikuchi, T. Namiki, I. Ikemoto, and K. Kobayashi, *J. Chem. Soc., Chem. Commun.*, **1986**, 1472.

24) K. Kobayashi, K. Kikuchi, T. Namiki, and I. Ikemoto, *Synth. Metals*, **19**, 555 (1986).

25) "International Tables for X-ray Crystallography, Vol. IV," ed by J. A. Ibers and W. C. Hamilton, Kynoch Press, Birmingham (1974).

26) T. Sakurai and K. Kobayashi, UNICS III, *Rep. Inst. Phys. Chem. Res.*, **55**, 69 (1979).

27) C. K. Johnson, ORTEP II, Report ORNL—3794, Oak Ridge National Laboratory, Tennessee, 1974.

28) K. Saito, H. Kamio, K. Kikuchi, K. Kobayashi, and I. Ikemoto, in preparation.

29) Tables of anisotropic temperature factors and $|F_o|-F_c$ data are deposited as Document No. 8924 at the Office of the Editor of Bull. Chem. Soc. Jpn.

30) K. Saito, Y, Ishikawa, K. Kikuchi, I. Ikemoto, and K. Kobayashi, *Acta Crystallogr., Sect. C*, **45**, 1403 (1989).

31) K. Mortensen, E. M. Conwell, and J. M. Fabre, *Phys. Rev. B*, **28**, 5856 (1983).

32) K. Miyazaki, K. Kikuchi, K. Saito, K. Kobayashi, and I. Ikemoto, unpublished.